Variable Capacity Air Source Heat Pump Coupled with a Building Integrated Photovoltaic/Thermal (BIPV/T) System

H. Getu[1,*] P. Dash, A. S. Fung[1],
[1]Department of Mechanical and Industrial Engineering, Ryerson University,
350 Victoria Street, Toronto, ON, Canada M5B 2K3

*corresponding author: ghailu@ryerson.ca, Tel. 1-416-979-5000, x 4097, FAX. 1-416-979-5265

Abstract

TRNSYS simulation software was used to evaluate the performance of a variable capacity air-to-air air source heat pump (VC-ASHP) coupled with a building integrated photovoltaic/thermal (BIPV/T) system. A known heat pump performance curve of an ASHP at a characterized test house was used in the simulation. The TRNSYS model was validated with the data collected from monitoring the VC-ASHP. From the results of the data collection, a curve was developed illustrating the daily heating output of the VC-ASHP with respect to the daily average outdoor temperature. This curve was used to validate the TRNSYS house model by matching the TRNSYS daily heating demand of the house at various daily average outdoor temperatures with the developed curve from the data. The BIPV/T system was integrated into the roof and the wall. Air was circulated behind the photovoltaic arrays to recover the thermal energy. The recovered warm air was supplied to the VC-ASHP. The thermal performance of the VC-ASHP was evaluated for three scenarios when the heat pump is running in heating mode. The three scenarios are: (A) by directly feeding ambient air to the ASHP; (B) by coupling the ASHP to a wall integrated BIPV/T only; and (C) by coupling the ASHP to a roof integrated BIPV/T only. The coefficient of performance (COP) of the VC-ASHP was evaluated for these three separate scenarios and compared. The COP was evaluated for three typical winter days: January 12, February 5 and March 5. Results suggest that the COP of the ASHP can be improved by coupling the VC-ASHP to either of the BIPV/T systems, i.e., either to the roof integrated BIPV/T system or to the wall integrated BIPV/T system.

Key words: Air source heat pump, TRNSYS, coefficient of performance (COP), solar energy, Building Integrated Photovoltaic/Thermal

Introduction

In Canada, buildings account for about 53% of electricity consumption, 30% energy consumption, and 33% of greenhouse gas emission (GHG) when primary energy generation is included in these estimates [1]. The GHG emission is even higher (55%) in large metropolitan areas such as Toronto and Vancouver [2, 3]. In Canada, 81% of the total household energy demand is for space and domestic water heating [4], which is usually achieved by combustion of natural gas in a hot air furnace or a water boiler. Some of the techniques of gas production, such as hydraulic fracturing, may contaminate nearby ground water resources [5] because during hydraulic fracturing, fluids containing chemicals are injected deep underground, where their migration is not entirely predictable [6]. The process of gas combustion generates GHG emission into the atmosphere. Large scale, fossil fuel-based energy generation systems can be replaced with distributed energy generation systems from renewable resources that have the potential to significantly lower environmental impacts. High efficiency technology supported by renewable resources has the potential to significantly lower electricity and thermal energy consumption produced from non-renewable resources.

Since the 1960s Photovoltaic (PV) modules have been used to generate electricity. The efficiency of the modules is greatly affected by heat, resulting in poor solar-to-electricity conversion [7, 8]. The efficiency can be improved by circulating fluid (air or water) behind the PV modules which removes the heat. Such hybrid Photovoltaic/Thermal (PV/T) systems not only improve the solar-to-electricity conversion but also provide thermal energy for heating the building. For these reasons PV/T systems have been a subject of interest since the mid-1970s [9, 10]. Early works [11-13] were aimed at validating the concept of PV/T through theoretical and experimental works. In the last 35 years the design and performance of PV/T systems has been significantly studied by many researchers [11-22]. In the 1990s, research focused on the collector design with the aim of improving the cost-performance ratio and energy and mass transfer phenomena analyses with experimental validation [23]. Chow [23] conducted a review of existing literature on PV/T and concluded that effective use of PV/T systems depended on geographical location. At locations with low levels of solar radiation and ambient temperatures, space heating is required much of the year and PV/T with air circulation can be useful and cost effective [23]. This finding is pertinent to the climatic conditions of Canada. In summary, a ventilated PV/T system was found to improve solar-to-electricity conversion with a possibility of extracting thermal energy, leading to a shorter payback time than the PV system alone.

Although PV/T systems that produce electricity and heat have been applied effectively on building roofs and facades to offset or eliminate fossil fuel demand in buildings, they were treated as separate and distinct systems from each other and from the building envelope with no significant reduction in payback time. The payback time can further be reduced by integrating a PV/T system to a building structure like façade or roof.

Building integrated photovoltaic (BIPV/T) systems are arrays of photovoltaic panels integrated into the building structures as facades and roofs that can produce electricity and useful thermal energy [24-28]. The recovery of the useful thermal energy is achieved by circulating air behind the PV arrays. This heat energy can be used for space and/or domestic water heating and even air conditioning. In this work, the warm air coming out of the BIPV/T system was fed to the ASHP and the COP was evaluated.

BIPV/T systems have the potential to meet all the building envelope requirements such as mechanical resistance and thermal insulation [25]. In addition to producing heat and electricity, the multiple functionality of BIPV/T system is expected to improve the cost effectiveness of residential construction as compared to add-on PV/T systems. PV/T systems are usually attached to the outer layer of the construction, requiring additional mounting systems [25]. The combination of BIPV/T system with a heat pump can further improve the thermal efficiency. It has been reported that the energy consumption of the ÉcoTerra house was only 26.8% of a typical Canadian home when a BIPV/T system was coupled with a geothermal heat pump [29]. The capital cost of a house with a BIPV/T system can further be reduced by coupling the system with an air source heat pump (ASHP) instead of ground source heat pump. Recent advances in two-stage variable capacity air source heat pump (TS VC ASHP) have demonstrated that such systems can successfully be used with comparable overall performance to ground source heat pump (GSHP). This is accomplished with less investment cost (only 40% of the cost of GSHP) even in the harsh Canadian climatic condition, cold in winter and hot in summer, without requiring any supplementary heat source even during the coldest period encountered at -22°C [30]. Due to the nature of the design, such ASHPs can be operated at extreme cold temperature utilizing the two-stage compression process at a lower coefficient of performance (COP) of approximately 1.5 while running first stage compression process at part-load most of the time with much higher COP of between 2 and 5 at outdoor temperature between -15 to 10 °C, resulting in an overall COP of approximately 3.0.

The objective of this work is to evaluate the performance of a VC-ASHP when it is coupled to a roof or wall integrated BIPV/T system. In order to facilitate this, a known performance curve of an ASHP at a characterized test house was used in the TRNSYS simulation. The coefficient of performance (COP) of the VC-ASHP will be evaluated for three separate scenarios and compared, for three typical winter days. The three scenarios are: (A) by supplying the ambient air directly to the ASHP (base case scenario); (B) by coupling the ASHP to the wall integrated BIPV/T only; and (C) by coupling the ASHP to the roof integrated BIPV/T only.

House Description

Archetype Sustainable Twin-Houses that were designed to demonstrate sustainable housing technologies were built at the Toronto and Region Conservation Authority's (TRCA) Kortright Centre for Conservation. The houses are one of the first Canadian projects to achieve a LEED for Homes Platinum Certification [28]. The left-hand side of the house, known as House A (Fig. 1), was analyzed in the current work. The house was designed to demonstrate current best practice sustainable technologies. It was designed to have an air-tight building envelope according to the standards of ASHRAE 90.1. The house has double glazed windows with fibreglass frames. Table 1 lists the structural features of the house and Table 2 lists its floor areas and zone volumes [30]. A two stage variable capacity air-to-air air source heat pump with 11.06 kW heating capacity, manufactured by Mitsubishi Electric (model PUZ-HA36NHA), with a direct expansion coil air handling unit for delivery of conditioned air, is used for space heating and cooling.

Fig. 1 South-west side of the twin house. In the current work, the left-hand side house (House A), indicated by the arrows, was analyzed.

Table 1: Structural features of the analyzed house (House A)

House part	Features
Basement walls	RSI 3.54 (R20)
Basement Slab	RSI 1.76 (R10)
Windows	2.19W/m2K (0.39 Btu/hr-ft2-°F
Roof	RSI 7 (R40)
Overall UA value	160 W/K

Table 2: Floor areas and zone volumes of the house

House part	Floor Area m^2 (ft^2)	Volume m^3 (ft^3)
Basement walls	86.95 (936)	234.03 (8264)
Basement Slab	86.95 (936)	291.54 (10296)
Windows	86.95 (936)	238.53 (8424)
Roof	83.6 (900)	222 (7840)
Total	344.45 (3708)	986.1 (34824)

House Internal Gains

The house was assumed to have four occupants (2 adults and 2 children). Load profiles of the house were created using incandescent light bulbs with schedules to represent the occupant internal gains [30]. Other gains within the house were measured depending on the type of equipment used [30]. Table 3 gives the internal heat gains for major appliances and lighting.

Table 3: Internal heat gains from equipment/appliance/lighting

	kWh/day	Annual kWh	kJ/hr
Interior lighting	3	1095	450
Major appliances	6	2190	900
Other	3	1095	450

TRNSYS Simulation

A transient system energy modeling software (TRNSYS) was used to evaluate the performance of the VC-ASHP coupled with the BIPV/T system. TRNSYS includes a graphical interface, a simulation engine, and a library of components that range from various building models to standard HVAC equipment to renewable energy. TRNSYS uses components known as Types connected to each other that form a system. Dynamic simulation is performed by TRNSYS to obtain the behavior of the system. TRNSYS is reasonably powerful in terms of HVAC system modeling [31].

The BIPV/T system was modeled using TRNSYS Type 568 component, which can operate with Type 56 multi-zone building with detailed zone models. Type 568 component (Fig. 2) is intended to model an un-glazed solar collector which has the dual purpose of creating power from embedded photovoltaic (PV) cells and providing heat to an air stream passing beneath the absorbing PV surface [32].

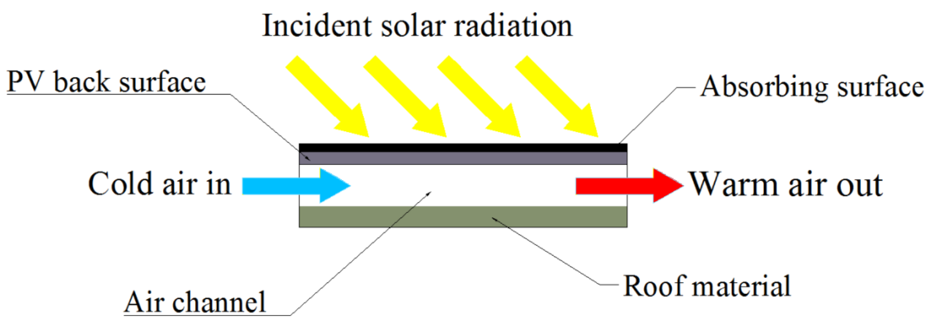

Fig. 2 Schematic of the collector.

Type 568 assumes the PV cells to be operating at their maximum power point condition. The thermal model of this collector is based on algorithms described by the Solar Engineering of Thermal Processes textbook by Duffie and Beckman [33]. In this model, set of energy balance equations are solved by iterative approach, initially by guessing the values for the mean fluid temperature, mean PV cell temperature, and mean air channel surface temperatures, until the solution converges.

The roof BIPV/T was placed on the southern part of the roof and mounted at 45°. The roof BIPV/T consisted of 25 panels (1m x 1.663m) placed 5x5 with air flowing from the base of the roof to the top. For thermal energy recovery, air was circulated through the steel roof channels under the PV by a 750 W fan. The corrugated roof channel depth was three inches. The channel width was twelve inches. For the wall BIPV/T, the southern wall consisted of a glass facade, an air gap (3 inches) and PV panel structure. The PV area on the wall was the same as the roof area, air flowing from the base of the house towards the roof. TRNSYS Type 687, a window model that uses the window's area, light transmittance, Solar Heat Gain Coefficient (SHGC), and U factor, and zone temperatures to predict the net gain through the window was used to model the glass facade.

In TRNSYS, for each component there are inputs, parameters, and outputs that can be linked to other components. The building model was created using information from House A. The HVAC systems were modeled based on the actual collected data. The house model was created using TRNBuild with known building envelope characteristics. The model was validated with the data collected from monitoring the VC-ASHP. From the results of the data collection, a curve was developed illustrating the daily cooling and heating output of the VC-ASHP with respect to the daily average outdoor temperature [30]. This curve was used to validate the TRNSYS house model by matching the TRNSYS daily heating demand of House A at various daily average outdoor temperatures with the developed curve from the data [30]. Fig. 3 shows the house heating validation where TRNSYS daily heating demand of the house at different daily average outdoor temperatures are matched with the daily ASHP heating at different daily average outdoor temperatures.

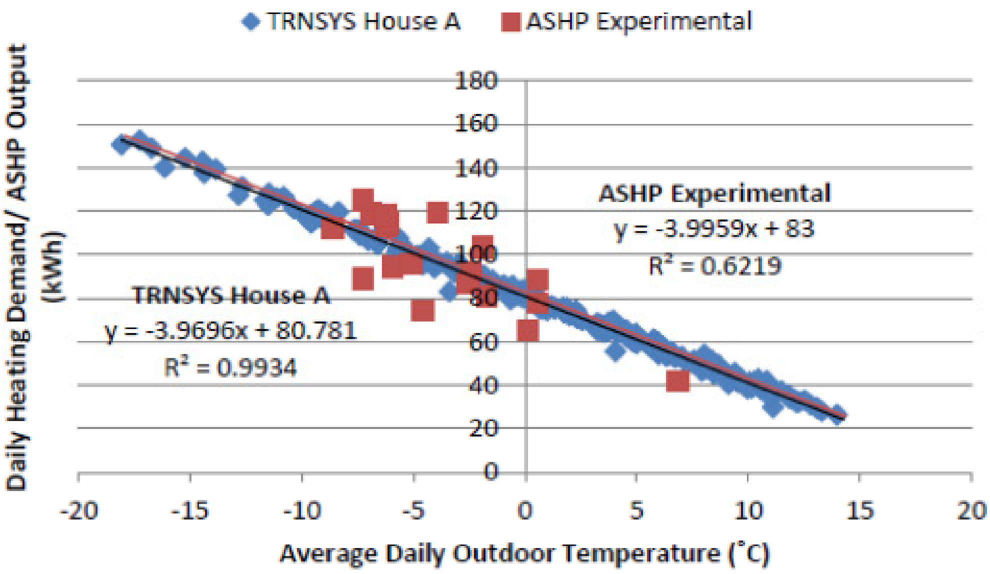

Fig. 3 TRNSYS House A heating validation.

Solar irradiation for the Greater Toronto Area (GTA) was used for the simulation (TMY2). For GTA, the heating season is from October 1st to April 30th. The simulation was run for the heating season only. The heating set point temperature was 21°C with a deadband temperature of 1.5 °C; and the thermostat was on the second floor of the house. The simulation was run with one minute time steps. The PV's electrical efficiency was assumed to be 15 % at a temperature of 25°C and the power output was assumed to decrease by 0.5% per 1°C increase in PV's temperature [34]. Absorptance of PV's surface and its emissivity were assumed to be 0.78 [35] and 0.95, respectively [36]. The steel roof properties were: thermal conductivity, 50 W/mK, specific heat capacity, 0.49kJ/kgK and density, 7850 kg/m^3.

Results and Discussion

The COP of the heat pump was calculated as the ratio of the output thermal energy to the input electrical consumption including the consumption of the 750W fan when the BIPV/T was coupled to the ASHP Three cases were investigated: Case A, base case scenario: when the ambient air is supplied directly to the heat pump; Case B: when the warm air coming out of the wall integrated BIPV/T is supplied into the heat pump and; Case C: when the warm air coming out of the roof integrated BIPV/T is supplied to the heat pump. The COP of the heat pump was evaluated for three winter days: January 12, February 05 and March 5.

Figure 4 shows the solar irradiation for January 12 from 7AM - 4PM. Figure 5 shows the temperature at the outlet of the roof integrated BIPV/T system, the wall integrated BIPV/T and the ambient temperature. From Fig. 5 it is seen that, around 11AM, the temperature at the out let of the BIPV/T reaches a maximum of 3 °C (around 20°C increase). This corresponds to the peak solar irradiation of the day. Around 11AM, by coupling the heat pump to the roof integrated BIPV/T system, the COP is increased from 1.8 to 4 corresponding to the maximum solar irradiation (or outlet temperature from the BIPV/T). The increase in COP is more than double. The wall integrated BIPV/T system coupled with the ASHP yields lower COP, 2.7.

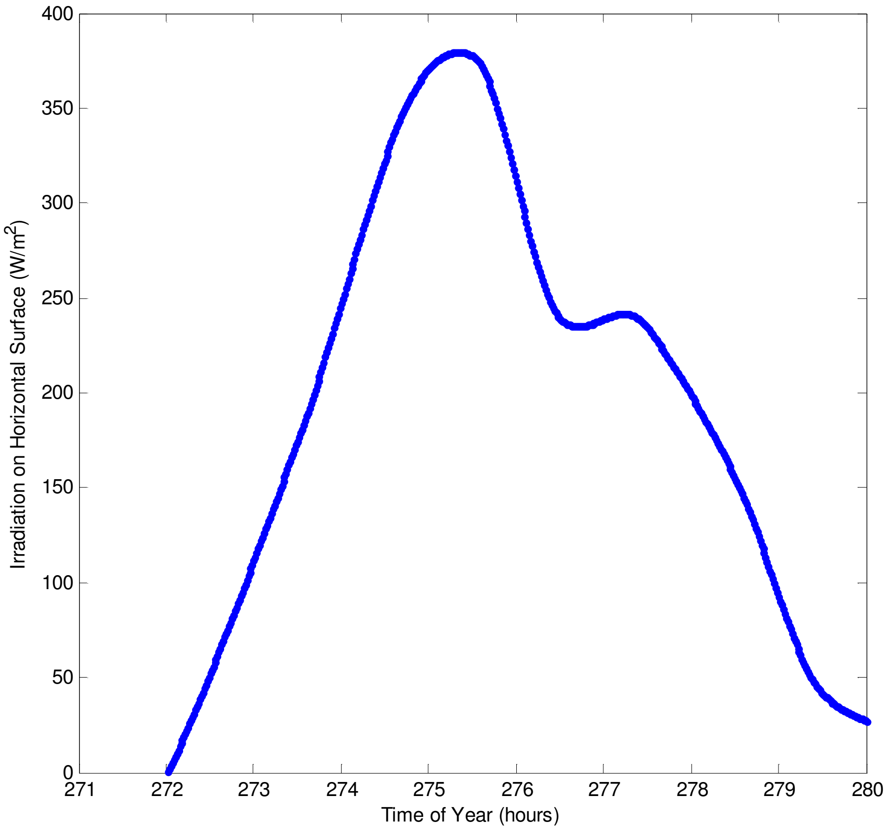

Fig. 4 Solar irradiation for January 12.

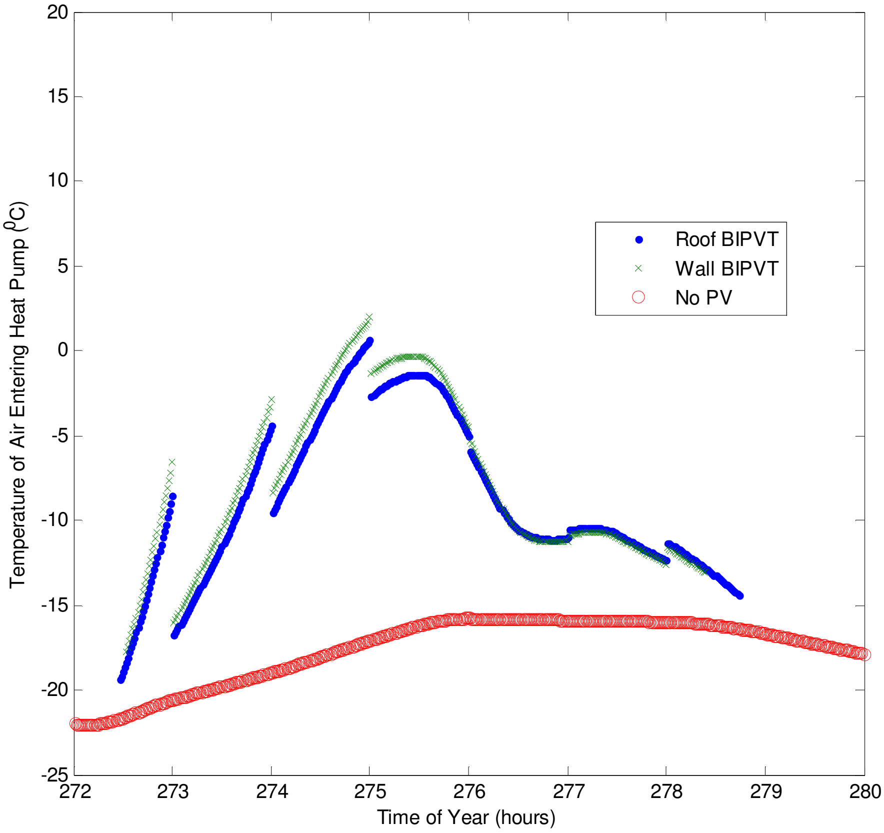

Fig. 5 Temperature profiles at the outlet of the BIPV/T systems for different cases.

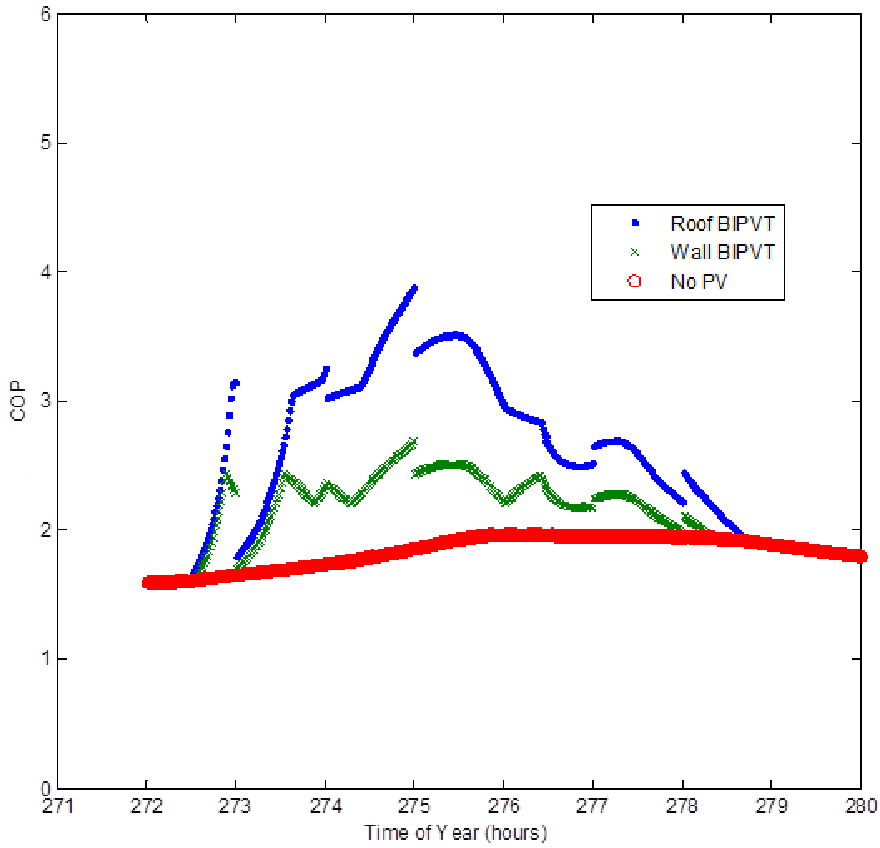

Fig. 6 COP of the ASHP for the three different cases.

Figure 7 shows the solar irradiation for February 05 from 9AM - 6PM. Figure 8 shows the temperature at the outlet of the roof integrated BIPV/T system, the wall integrated BIPV/T and the ambient temperature. From Fig 8 it is seen that the temperature at the out let of the BIPV/T can be increased by a maximum of 13 °C corresponding to the peak solar irradiation of the day around 11:30AM. Around this time both the roof and wall integrated BIPV/T systems yield the same outlet temperature. After this time the wall integrated BIPV/T system does not yield warmer air temperatures as compared to the ambient air. Around 11:30AM, by coupling the heat pump to the roof integrated BIPV/T system, the COP is increased from 3 to 4.5 (Fig. 9) corresponding to the maximum solar irradiation (or outlet temperature from the BIPV/T). Around 11:30AM the wall integrated BIPV/T system yields very little increase in COP, from 3.0 (base case scenario) to 3.2.

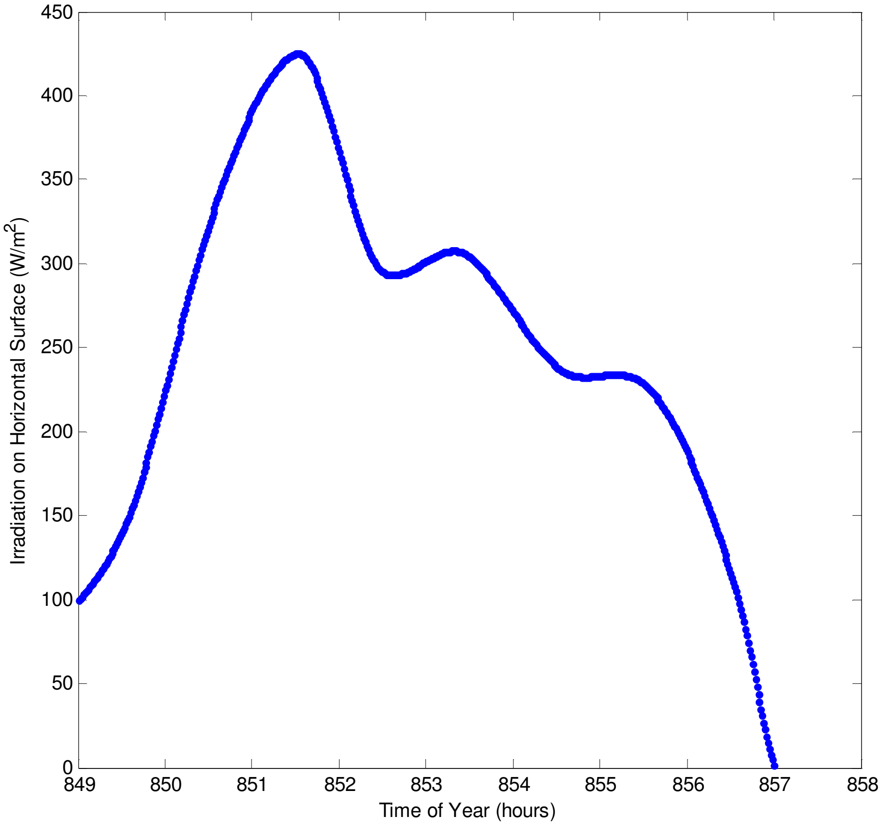

Fig. 7 Solar irradiation for February 5.

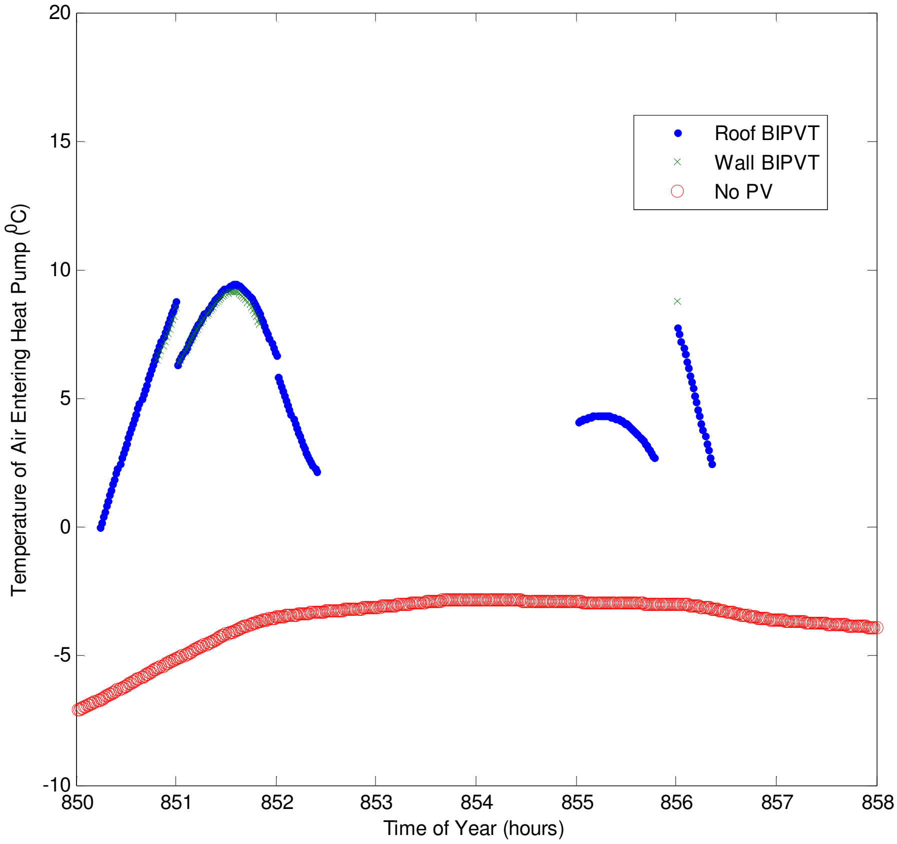

Fig. 8 Temperature profiles at the outlet of the BIPV/T systems for different cases.

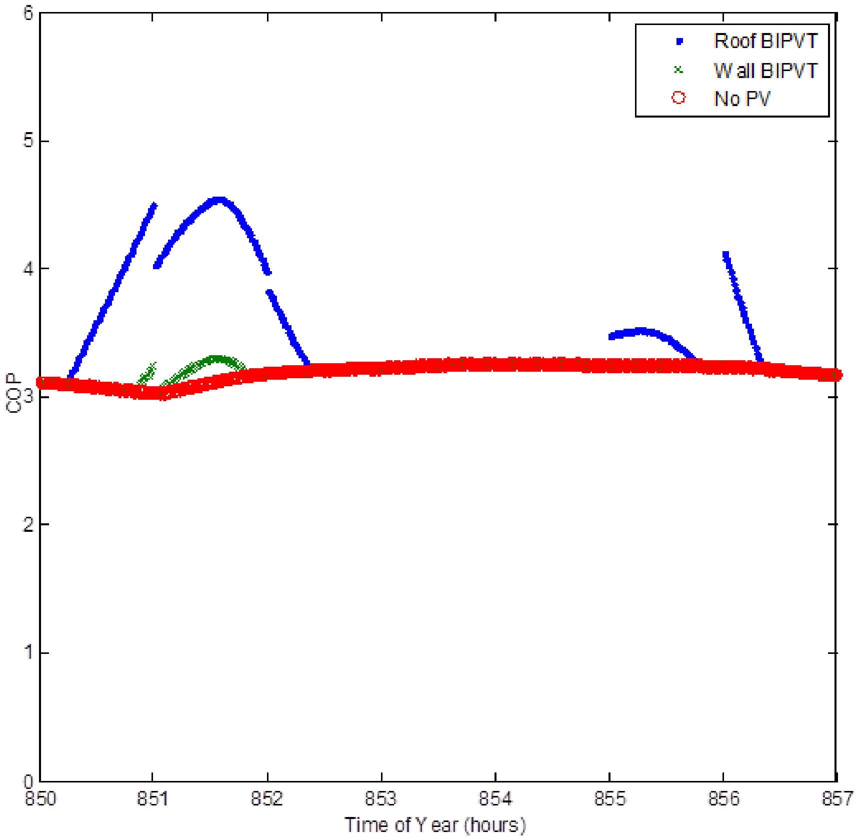

Fig. 9 COP of ASHP for the three different cases.

Figure 10 shows the solar irradiation for March 5 from 7AM - 4PM. Figure 11 shows the temperature at the outlet of the roof integrated BIPV/T system, the wall integrated BIPV/T and the ambient temperature. From Fig 11 it is seen that the temperature at the outlet of the roof integrated BIPV/T can be increased by a maximum of 15 °C corresponding to the peak solar irradiation of the day around 9:30AM. Around 9:30 AM, by coupling the heat pump to the roof integrated BIPV/T system, the COP is increased from 3.2 to 4.6 (Fig. 12) corresponding to the maximum solar irradiation (or outlet temperature from the BIPV/T).

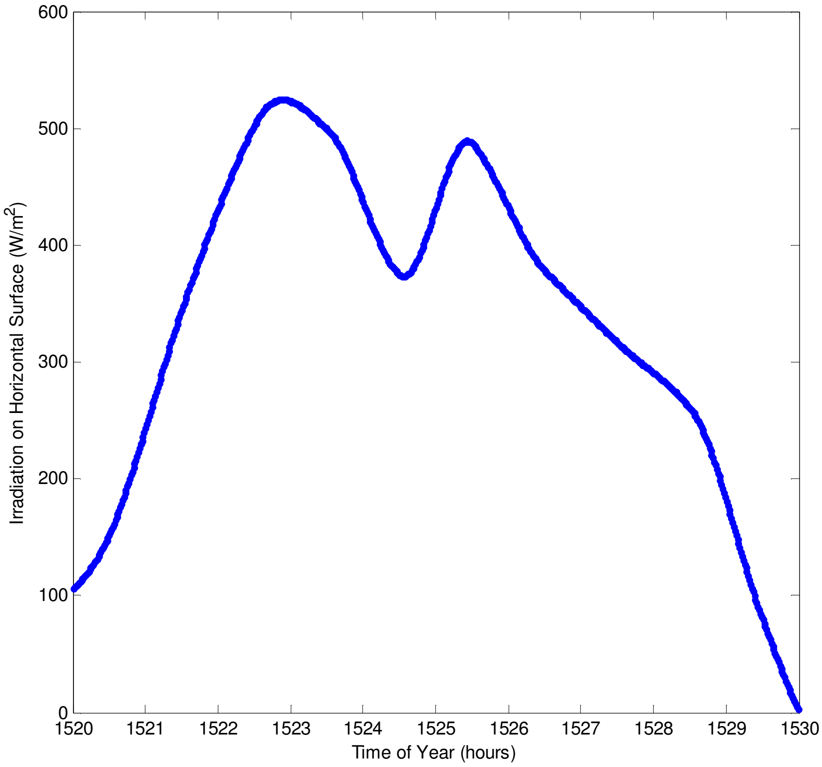

Fig. 10 Solar irradiation for March 5.

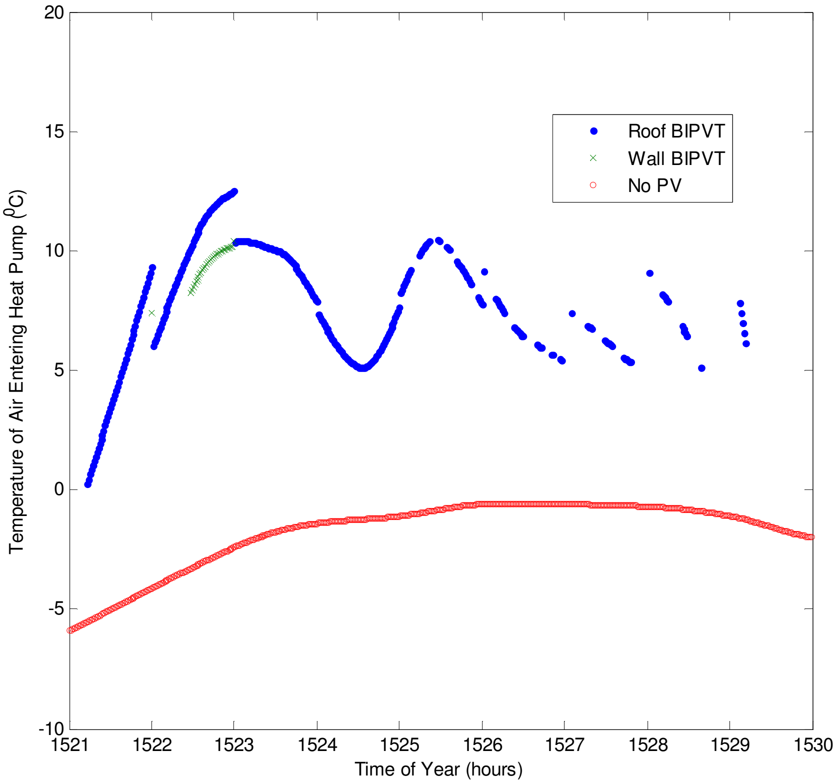

Fig. 11 Temperature profiles at the outlet of the BIPV/T systems for different cases.

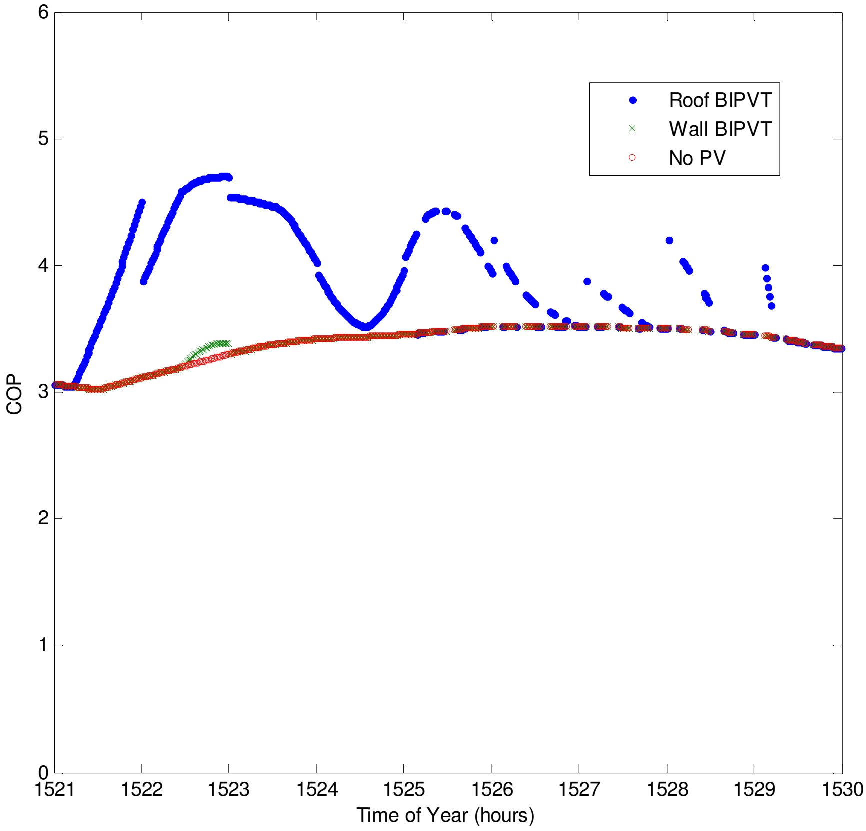

Fig. 12 COP of ASHP for the three different cases.

The COP of the ASHP was also calculated by assuming that thermal energy recovery is achieved by circulating air using the heat pump fan alone, i.e. no additional fan is required. This results in less power consumption. Fig. 13 to Fig. 15 show the COP of the ASHP for three different days assuming this situation. In general, the ASHP's COP is enhanced by coupling it with either wall integrated and roof integrated BIPV/T systems, which was not the case when additional fan was used to circulate the air. When additional fan was used, there was no much enhancement in the COP of the ASHP when it was coupled with wall integrated BIPV/T systems for February and March days.

From Fig. 13 it is seen that the COP of the ASHP reaches a maximum of 3.8 from 1.8 for January 12, by coupling the ASHP to either the wall or roof integrated BIPV/T system. This corresponds to the maximum solar irradiation (or outlet temperature from the BIPV/T). The increase in COP is more than double. Figure 14 shows that the COP of the ASHP is increased from 3 to 5.4, corresponding to the maximum solar irradiation (or outlet temperature from the BIPV/T), by coupling the ASHP to the roof integrated BIPV/T system. When the ASHP is coupled to the wall integrated BIPV/T, it yields slightly less COP in comparison to the ASHP coupled with the roof integrated BIPV/T for this day. From Fig. 15 it is seen that the COP of the ASHP coupled with the roof integrated BIPV/T system is increased from 3.5 to 5.2

corresponding to the maximum solar irradiation (or outlet temperature from the BIPV/T) for March 15. For this day the ASHP coupled with the wall integrated BIPV/T yields less COP throughout the day.

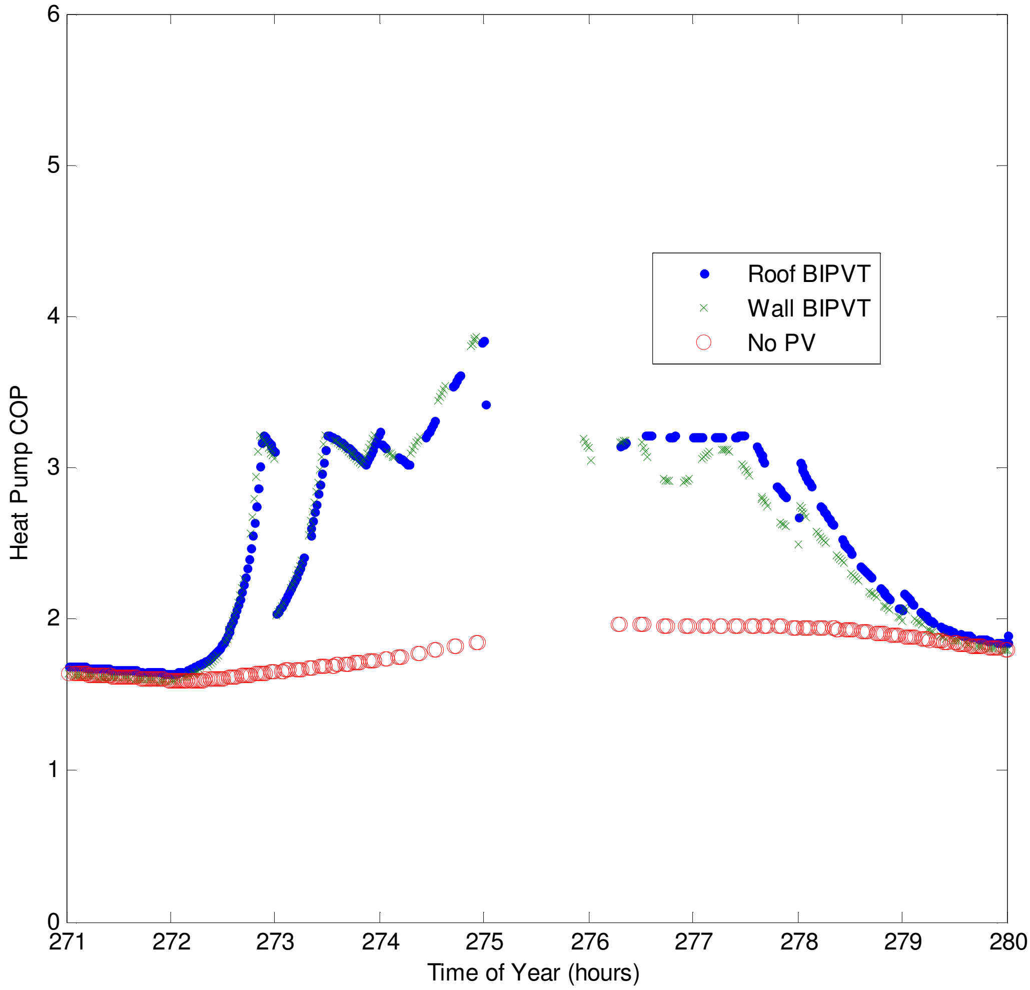

Fig. 13 COP of the ASHP for the three different cases for January 12.

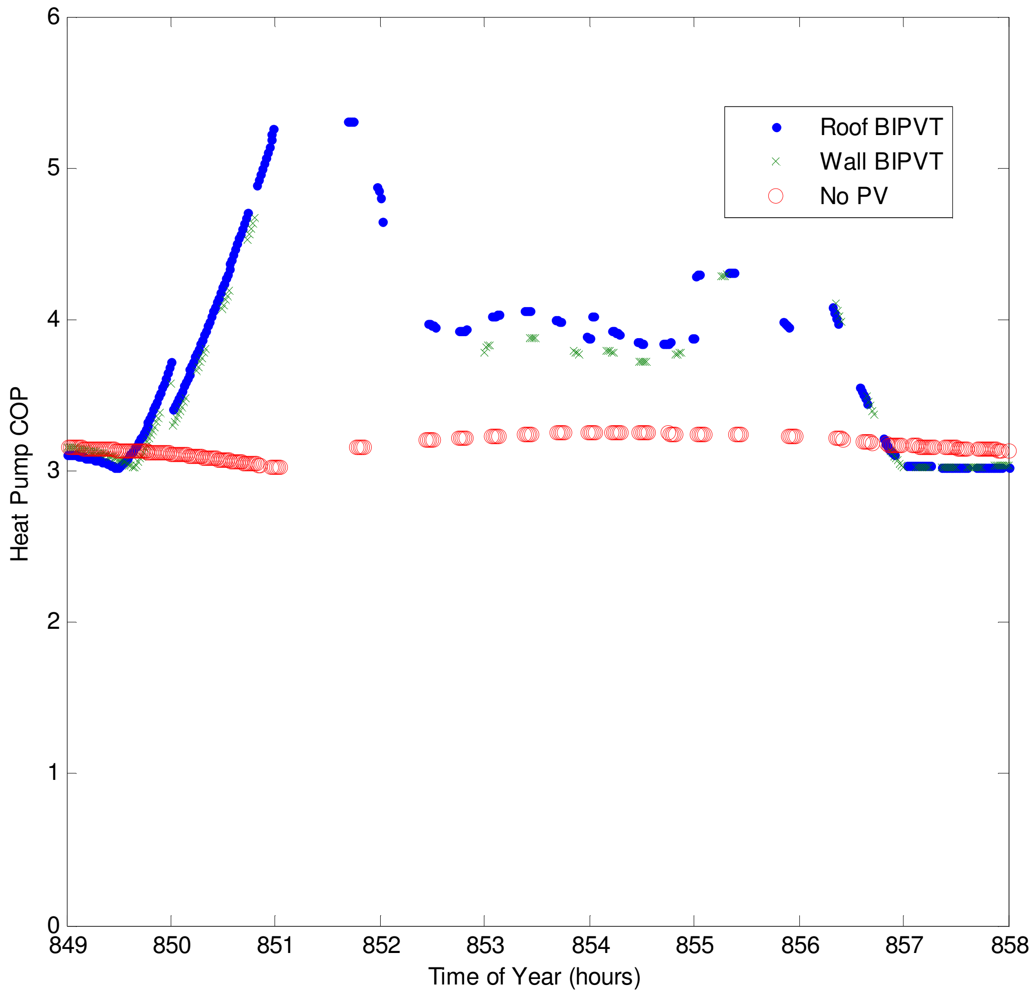

Fig. 14 COP of ASHP for the three different cases for February 5.

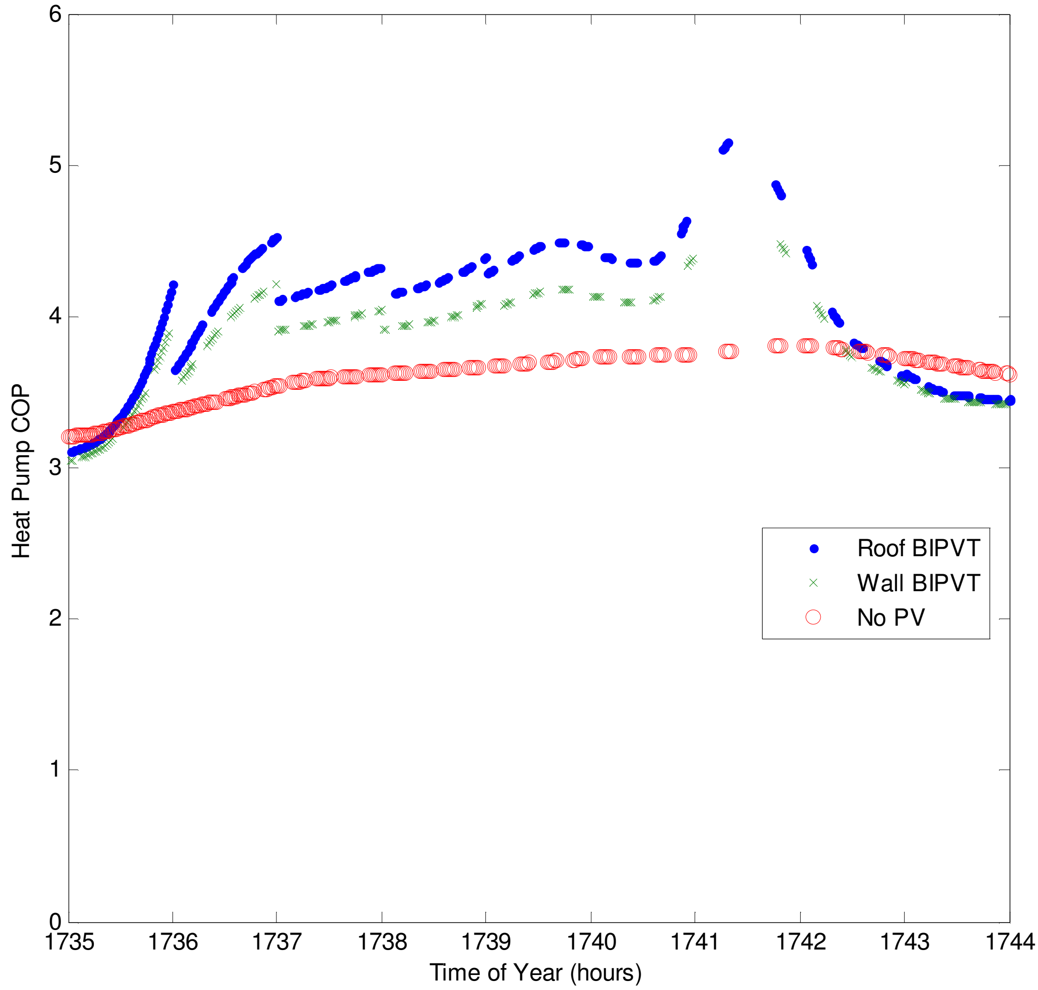

Fig. 15 COP of ASHP for the three different cases for March 15.

Seasonal COP

Figure 16 compares the COP of the heat pump for the base case scenario with the COP of the heat pump when it is coupled with roof integrated BIPV/T system for three months, January 1 to March 31. It is seen from the Fig. 16 that, generally, the COP of the heat pump is increased when it is coupled with the roof integrated BIPV/T system.

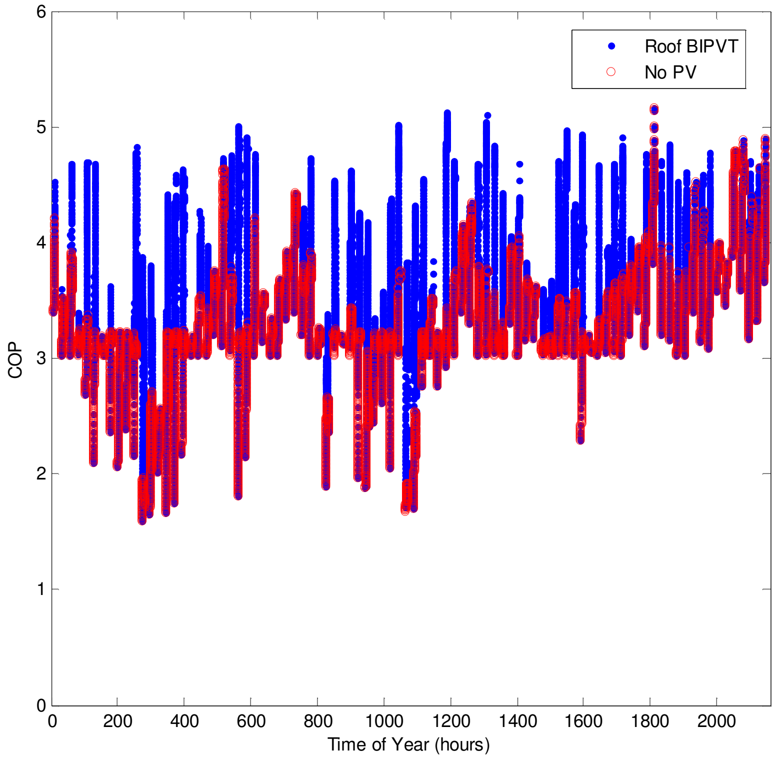

Fig. 17 COP of the heat pump when coupled with the roof integrated BIPV/T system for three months (January 1 to March 31).

Fig. 14 compares the COP of the heat pump for the base case scenario with the COP of the heat pump when it is coupled with wall integrated BIPV/T system for three months, January 1 to March 31. There is slight increase in the COP of the heat pump when it is coupled to the wall integrated BIPV/T system. However, it is noted that no preheat was considered for this case. It has been reported that there is on average 4.4°C difference between the inlets temperature to the roof integrated BIPV/T and the ambient temperature [37]. Since it is not known if there is preheating of the wall integrated BIPV/T systems, it was not included in this work.

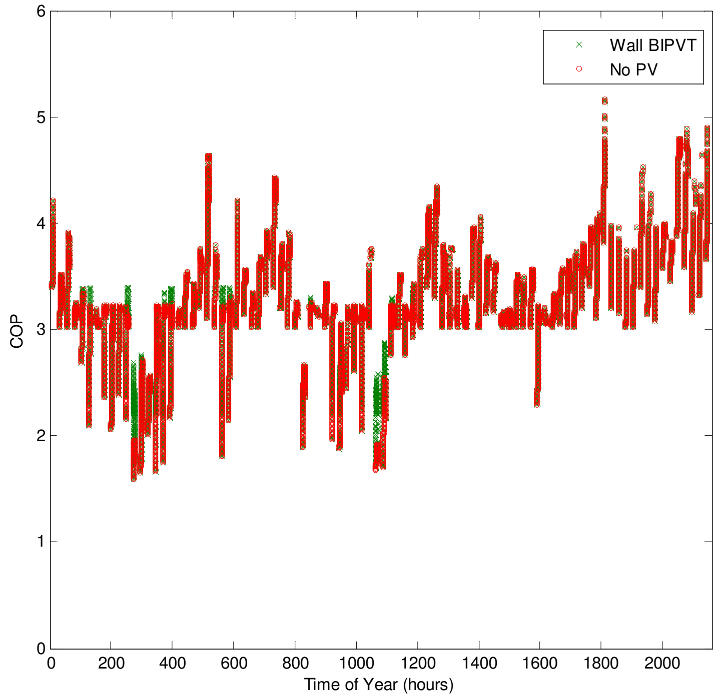

Fig. 18 Seasonal COP of the heat pump when coupled with the wall integrated BIPV/T system for three months (January 1 to March 31).

Conclusion

A validated TRNSYS simulation was used to evaluate performance of a variable capacity air-to-air air source heat pump (VC-ASHP) under three different conditions: (A) by feeding the ambient air to the ASHP; (B) by coupling the ASHP to the wall integrated BIPV/T only and (C) by coupling the ASHP to the roof integrated BIPV/T only. Results of typical winter days were compared for these three cases and it was found that coupling the ASHP to either the roof or wall integrated BIPV/T systems improves the COP of the heat pump when the heat pump fan is used to recover the thermal energy. The seasonal COP is improved when the ASHP is coupled to the roof integrated BIPV/T system.

Acknowledgments

The authors gratefully acknowledge the financial support of the Natural Sciences and Engineering Research Council of Canada (NSERC), Toronto Atmospheric Fund (TAF), MITACS and Ryerson University.

References

[1]http://www.nsercpartnerships.ca/How-Comment/Networks-Reseaux/SNEBSN-BICENN-eng.asp, accessed Oct. 02 2013.
[2] NRCan 2006, Energy Use Data Handbook, http://oee.nrcan.gc.ca/publications/statistics/handbook06/pdf/handbook06.pdf, accessed Oct 01 2013
[3] W. Knowles, The myths and realities of real building energy performance, Market Insight Event-Existing Buildings: Addressing Performance from the Outside, May 01 2011.
[4] C. Aguilar, D.J. White and D. L. Ryan (2005). Domestic water heating and water heater energy consumption in Canada, Canadian Building Energy End-Use Data and Analysis Centre. CBEEDAC 2005–RP-02.
[5] D. C. DiGiulio, R.T. Wilkin, C. Miller and G. Oberley (2011). Investigation of ground water contamination near Pavillion, Wyoming. US EPA report.
[6] H. Waxman, A. E. J. Markey and D. DeGette (2011). Chemicals used in hydraulic fracturing. Report of Committee on Energy and Commerce U.S. House of Representatives.
[7] L. Devarakonda and S. Mil'shtein (2012). Limiting Solar Cell Heat-Up by Quantizing High Energy Carriers. ISRN Renewable Energy, Volume 2012, Article ID 862790, 5 pages.
[8] L. Zhang, D. Jing, L. Zhao, J. Wei and L. Guo (2012). Concentrating PV/T Hybrid System for Simultaneous Electricity and Usable Heat Generation: A Review. International Journal of Photoenergy, Volume 2012, Article ID 869753, 8 pages.
[9] L.W. Florschuetz (1975). On heat rejection from terrestrial solar cell arrays with sunlight concentration. Proceedings of the 11th IEEE PVSC conference. New York, USA, 318–326.
[10] M. Wolf (1976). Performance analysis of combined heating and photovoltaic power systems for residences. Energy Conversation 16 (1-2): 79–90.
[11] L.W. Florschuetz (1979). Extension of the Hottel–Whiller model to the analysis of combined photovoltaic/thermal flat plate collectors. Solar Energy 22: 361–366.
[12] J.E.C Kern and M.C. Russell (1978). Combined photovoltaic and thermal hybrid collector Systems, Proceedings of the 13th IEEE photovoltaic specialists. Washington DC, USA1153–7.
[13] S.D. Hendrie (1979). Evaluation of combined photovoltaic/thermal collectors. Proceedings of the ISES international congress, Atlanta, USA, vol. 3: 1865–9.
[14] H.A. Zondag (2008). Flat-plate PV-Thermal collectors and systems: a review. Renewable and Sustainable Energy Reviews 12 (4):891–959.
[15] P. Raghuraman (1981). Analytical prediction of liquid and air photovoltaic/thermal flat plate collector performance. Journal of Solar Energy Engineering 103 (16-21): 291–298.
[16] E. Skoplaki and J.A Palyvos (2009). On the temperature dependence of photovoltaic module electrical performance: a review of efficiency/power correlations. Solar Energy 83 (5): 614–624.
[17] Y. Tripanagnostopoulos (2007). Aspects and improvements of hybrid photovoltaic/thermal solar energy systems. Solar Energy 81 (9): 1117–31.
[18] A. Braunstein and A. Kornfeld (1986). On the development of the solar photovoltaic and thermal (PVT) collector. IEEE Trans Energy Convers, EC-1(4): 31–33.
[19] B. Lalovic (1986). A hybrid amorphous silicon photovoltaic and thermal solar collector. Solar Cells 19 (2):131–138.
[20] M.J. O'leary and L.D. Clements (1980). Thermal–electric performance analysis for actively cooled, concentrating photovoltaic systems. Solar Energy 25 (5): 401–406.
[21] D.J. Mbewe, H.C. Card and D.C Card (1985). A model of silicon solar cells for concentrator photovoltaic and photovoltaic/thermal system design. Solar Energy 35 (3): 247–258.

[22] S.J. Anand, D. Ibrahim and V.R. Bale (2009). Performance analysis of photovoltaic systems: a review. Renewable and Sustainable Energy Review 13 (8): 1884–97.
[23] T. Chow (2010). A review on photovoltaic/thermal hybrid solar technology. Applied Energy 87 (2), 365–79.
[24] Y. Chen, A.K. Athienitis, K.E. Galal, and Y. Poissant (2007). Design and Simulation for a Solar House with BIPV/T System and Thermal Storage. ISES Solar World Congress, Beijing, China, Vol. I, 327-32.
[25] Y. Chen, A.K. Athienitis, K.E. Galal (2010). Modeling, design and thermal performance of a BIPV/T system thermally coupled with a ventilated concrete slab in a low energy solar house: Part 1, BIPV/T system and house energy concept. Solar Energy 84(11): 1892-907.
[26] Y. Chen, K. Galal and A. K. Athienitis (2010). Modeling, design and thermal performance of a BIPV/T system thermally coupled with a ventilated concrete slab in a low energy solar house: Part 2 ventilated concrete slab. Solar Energy 84(11): 1908-19.
[27] J. Candanedo and A.K. Athienitis (2008). Simulation of the Performance of a BIPV/T system coupled to a Heat Pump in a Residential Heating Application. Proc. of the 9th International Heat Pump Conference, Zürich, Switzerland.
[28] A. Dembo, A. Fung, K.L.R. Ng and A. Pyrka (2010). The Archetype Sustainable House: Investigating its potentials to achieving the net-zero energy status based on the results of a detailed energy audit. International High Performance Buildings Conference 2010, Purdue University, 3247.
[29] M. Doiron, W. O'Brien and A. A. Athienitis (2011). Energy performance, comfort and lessons learned from a near net-zero energy solar house. ASHRAE Transactions 2011 (117): 585–596.
[30] A. A. Safa (2012). Performance Analysis of A Two-stage Variable Capacity Air Source Heat Pump and A Horizontal Loop Coupled Ground Source Heat Pump System. MASc thesis, Mechanical and Industrial Engineering, Ryerson University.
[31] D. Crarley, J. Hand, M. Kummert & B. Griffith (2005). Contrasting the Capabilities of Building Energy Performance Simulation Programs. Washington, United States of America.
[32] TRNSYS 16 Manual
[33] John A. Duffie*,* William A. Beckman, Solar Engineering of Thermal Processes. Wiley, 1980.
[34] Green, Martin A. Solar Cells: Operating Principles, Technology, and System Applications. Englewood Cliffs, NJ: Prentice-Hall, 1982.
[35] T.N. Anderson, M. Duke, G.L. Morrison, and J.K. Carson (2009). Performance of a Building Integrated Photovoltaic/thermal (BIPVT) Solar Collector. *Solar Energy* 83 (4): 445-55.
[36] Planning and Installing Solar Thermal Systems: A Guide for Installers, Architects and Engineers. James & James/Earthscan, London 2010.
[37] Doiron A. Matthew (2011). Whole Building Energy Analysis and Lessons Learned for a Near Net Zero Energy Solar House, MASc. Thesis, Concordia University.